Journal of Power Sources 196 (2011) 2871–2874

Contents lists available at ScienceDirect

Journal of Power Sources

journal homepage: www.elsevier.com/locate/jpowsour

Short communication

Template-assisted synthesis of high packing density $SrLi_2Ti_6O_{14}$ for use as anode in 2.7-V lithium-ion battery

Damien Dambournet*, Ilias Belharouak*, Jiwei Ma, Khalil Amine

Chemical Sciences and Engineering Division, Argonne National Laboratory, 9700 South Cass Avenue, Argonne, IL 60439, USA

ARTICLE INFO

Article history:
Received 4 October 2010
Received in revised form 2 November 2010
Accepted 3 November 2010
Available online 9 November 2010

Keywords:
Template
Anode
Li-ion batteries
$SrLi_2Ti_6O_{14}$

ABSTRACT

$SrLi_2Ti_6O_{14}$ has been prepared by using mesoporous TiO_2 brookite as a template and reactant. The prepared particles retained the rounded shape of the precursor, leading to high dispersivity and high packing density. The material has been further electrochemically characterized in both half and full cells. It shows good cycling stability and rate capability. A 2.7-V cell has been built by combining a $SrLi_2Ti_6O_{14}$ anode with a 4-V spinel cathode of $LiMn_2O_4$. This cell has a higher voltage compared to the 2.5-V $LiMn_2O_4/Li_4Ti_5O_{12}$ system.

1. Introduction

The safety concern related to the use of a carbonaceous-based electrode in lithium-ion batteries (LIBs) has driven ample research directed toward improving the cell abuse tolerance via engineering and cell chemistry solutions. Within the latter approach, the use of less reducing anodes can mitigate the thermal instability of the solid-electrolyte interface, thus improving the safety of the battery. Titanium-based oxides, including the commercially available $Li_4Ti_5O_{12}$, are suitable anodes because they operate at 1.5–1.8 V within the electrolyte stability zone [1]. Nevertheless, it is of interest to investigate other systems that can display a lower operating voltage in order to increase the overall energy density of the cell while operating within the electrolyte stability region. In this regard, the complex titanates $SrLi_2Ti_6O_{14}$ and $BaLi_2Ti_6O_{14}$ were considered as potential candidates to replace $Li_4Ti_5O_{12}$ due to their low operating voltage, around 1.3–1.4 V [2]. Later, $Na_2Li_2Ti_6O_{14}$ was reported to display an even lower potential of 1.25 V [3]. A comparative study of sol-gel synthesized $MLi_2Ti_6O_{14}$ (M = Ba, Sr, 2Na) compounds has shown that $SrLi_2Ti_6O_{14}$ exhibited the most promising properties [4]. Additionally, these materials possess less inactive lithium atoms as compared to $Li_4Ti_5O_{12}$, which can help reducing the cost, especially if an "all electric" vehicle is to be developed [5].

The synthesis of complex metal oxides with a defined shape is challenging, mostly because of the calcination at high temperature that is required for the preparation of pure crystalline phases. High temperature calcinations often lead to the formation of agglomerates, which prevent the growth of well-defined particles. Template-directed synthesis is a powerful route to tune the morphology and, hence, the physical properties of advanced materials. This technique has been widely used for the preparation of electrode materials using soft and hard templates [6]. An alternative to the use of organic (surfactants, co-polymer, etc.) or inorganic membranes (anodic aluminum oxide, silica, etc.) is a template that combines a pre-existing and well-defined shape structure and also plays the role of a chemical reagent. Such a method was presently adopted for the preparation of the complex titanate $SrLi_2Ti_6O_{14}$ by using mesoporous TiO_2 with a well-defined shape as both a template and reactant. Recently, we reported on the synthesis of mesoporous TiO_2 brookite prepared by thermal decomposition of an oxalate precursor obtained by an aqueous precipitation method [7].

Criteria for the selection of an electrode material are tightly related to its morphology. For high rate performance, nano-structured materials are undoubtedly more suitable than micron-sized particles. Nevertheless, nano-particles display several drawbacks related to their tendency to form agglomerates, leading to inhomogeneous electrodes. On the contrary, micron-sized and well-defined particles, especially rounded ones, exhibit a better dispersibility and, more important, have higher volumetric energy density. In the present work, mesoporous and micron-size particles of TiO_2 were used as a template for the synthesis of the complex titanate $SrLi_2Ti_6O_{14}$. The latter was characterized for use as the anode for lithium-ion batteries.

* Corresponding authors. Tel.: +1 630 252 4450; fax: +1 1630 252 5528.
E-mail addresses: dambournet@anl.gov (D. Dambournet), belharouak@anl.gov (I. Belharouak).

0378-7753/$ – see front matter © 2010 Published by Elsevier B.V.
doi:10.1016/j.jpowsour.2010.11.011

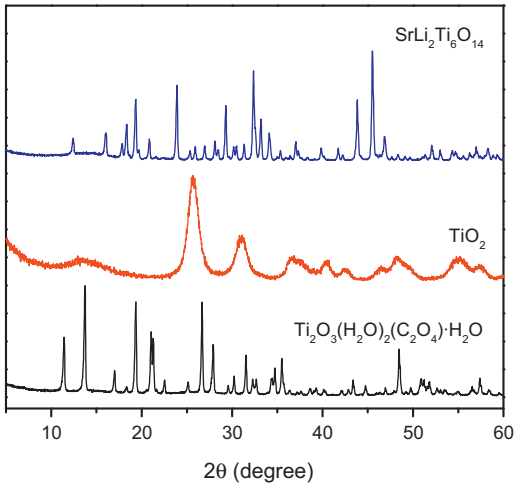

Fig. 1. X-ray diffraction powder patterns of $Ti_2O_3(H_2O)_2(C_2O_4)\cdot H_2O$, TiO_2 brookite, and $SrLi_2Ti_6O_{14}$.

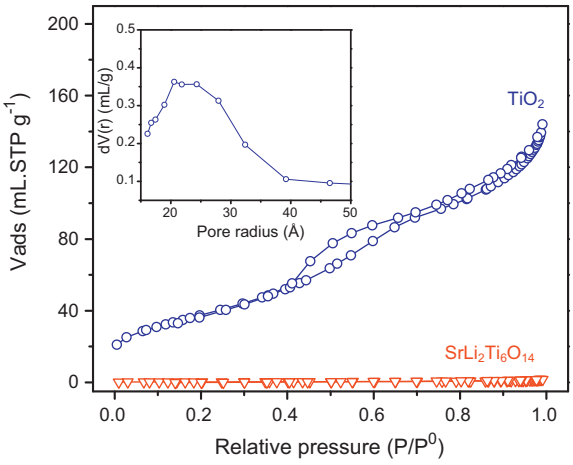

Fig. 3. N_2 adsorption isotherms of TiO_2 and $SrLi_2Ti_6O_{14}$. *Inset*: Radius pore size distribution for TiO_2.

2. Experimental procedure

A two-step process was used for the synthesis of $SrLi_2Ti_6O_{14}$. First, the TiO_2 precursor, the oxalate-based compound $Ti_2O_3(H_2O)_2(C_2O_4)\cdot H_2O$, was synthesized by an aqueous precipitation method performed at 90 °C for 3 h. Titanium oxysulfate (Sigma–Aldrich, Supelco) and $Li_2C_2O_4$ were used as chemicals. After washing and drying the titanium oxalate hydrate, it was decomposed at 400 °C, leading to pure TiO_2. Thereafter, TiO_2 was dispersed in an ethanol/acid acetic solution containing the strontium acetate and lithium acetate dihydrate (Sigma–Aldrich) initially dissolved. The mixture was then evaporated until dryness. The obtained powder was calcined at 900 °C for 12 h under an air atmosphere. In addition, $LiMn_2O_4$ was synthesized by using stoichiometric proportions of $MnCO_3$ and Li_2CO_3 calcined at 800 °C.

The titanate samples were characterized by various methods. Powder X-ray diffraction (XRD) was performed with a Siemens D5000 diffractometer (Cu-Kα). Scanning electron microscopy (SEM, Hitachi S-4700-II) was performed at the Electron Microscopy Center of Argonne National Laboratory. The packing density was measured by a standard method using an Autotap instrument from Quantachrome Instruments. Nitrogen adsorption isotherms were recorded at 77 K on a NOVA 2200e instrument. A powder sample (200 mg) was evacuated at 200 °C overnight prior to N_2 adsorption. The specific surface area was calculated by the Brunauer–Emmett–Teller (BET) method applied in the relative pressure (P/P^0) range between 0.04 and 0.29. The pore size distribution was determined by means of the Barrett–Joyner–Halenda algorithm using the adsorption branch.

Electrochemical measurements were carried out with CR2032-type coin cells. The composition of the electrode was 80 wt.% active materials, 10 wt.% acetylene black, and 10 wt.% polyvinylidene difluoride. Copper was used as the current collector. The electrolyte was 1.2 M $LiPF_6$ dissolved in a mixture of ethylene carbonate and ethyl methyl carbonate (3:7, v/v). The cells were assembled with lithium metal as the anode and were tested in the voltage range of 0.5–2 V at different current densities.

3. Results and discussion

The synthesis conditions were selected to achieve rounded and micron-sized TiO_2 particles offering suitable dispersibility and high packing density. X-ray diffraction analysis (Fig. 1) confirmed the phase purity of the oxalate phase whose pattern was indexed within the Cmca space group [8]. After thermal decomposition at 400 °C, the titanium oxalate phase transformed to TiO_2 brookite, as confirmed by XRD (Fig. 1). Due the removal of the oxalate/water species during the decomposition of $Ti_2O_3(H_2O)_2(C_2O_4)\cdot H_2O$, mesoporosity was created within the particle while the micron-sized feature of the precursor particles was retained after decomposition (Fig. 2). Nitrogen adsorption/desorption performed on the formed TiO_2 displays

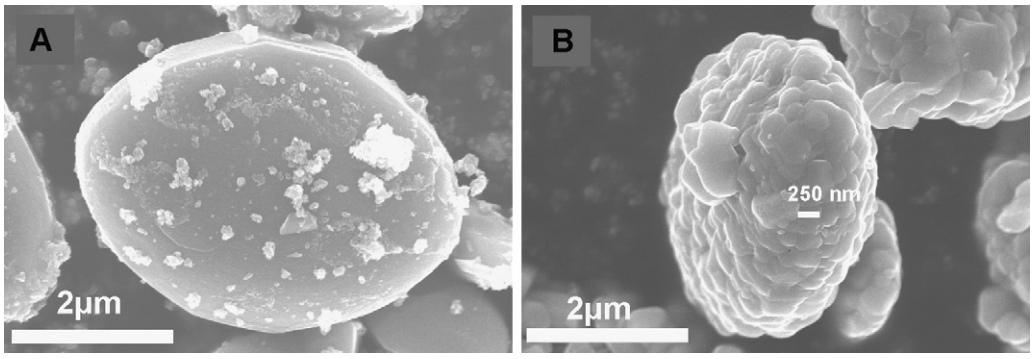

Fig. 2. Scanning electron microscopy images of TiO_2 precursor (A) and $SrLi_2Ti_6O_{14}$ (B).

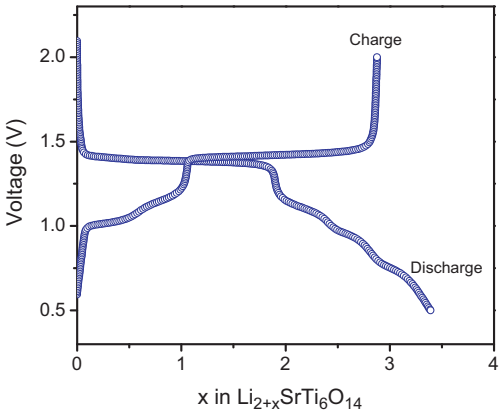

Fig. 4. First discharge/charge curves for $SrLi_2Ti_6O_{14}$/Li half cell cycled at 10 mA g^{-1} current density.

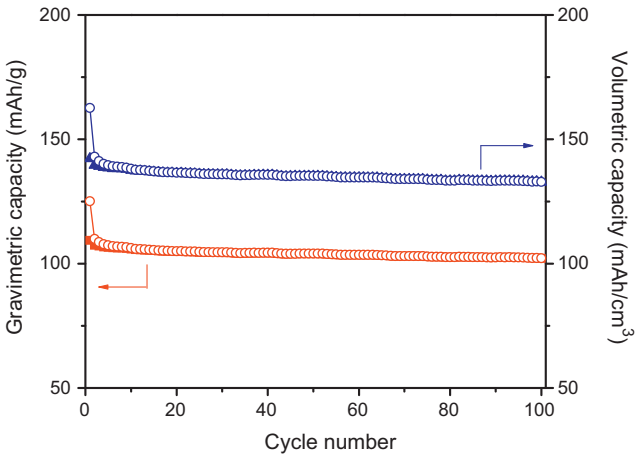

Fig. 5. Gravimetric and volumetric capacity of $SrLi_2Ti_6O_{14}$/Li half cell cycled at 100 mA g^{-1} (~1 C rate) current density. The first three cycles were performed at 10 mA g^{-1}.

a typical type IV isotherm characteristic of mesoporous materials (Fig. 3). The specific surface area calculated from the BET method was 138 m^2 g^{-1} confirming the porosity of the particles. The radius pore size distribution (Fig. 3, inset) obtained by the Barrett–Joyner–Halenda algorithm presented a maximum at 21 Å. During the impregnation process of TiO_2, the pores of the particles can be filled with the solution containing the additional elements, i.e., lithium and strontium, enabling a homogeneous dispersion and a closer contact of every reactant within the particle. The obtained mixture was calcined at a temperature as high as 900 °C to ensure the production of a pure and crystalline phase and to prove the concept of template-assisted synthesis. A comparison between the morphology of the TiO_2 precursor and the prepared $SrLi_2Ti_6O_{14}$ revealed that the micron size of the particles was maintained (Fig. 2). Additionally, the crystallization/growth processes occurred within the starting TiO_2 particles, leading to the formation of fused sub-micron crystallites embedded in the micron-sized particles. Although SEM analysis revealed the presence of few aggregates, most of the formed particles were well dispersed. The measured specific surface area of $SrLi_2Ti_6O_{14}$ was 1 m^2 g^{-1}, indicating the fusing of the particles pores during the formation of $SrLi_2Ti_6O_{14}$. From TiO_2 to $SrLi_2Ti_6O_{14}$, the packing density increased from 1 to 1.3 g cm^{-3}, the latter being on the higher end for titanium-based anode materials.

Fig. 4 shows the first discharge and charge curves obtained for a $SrLi_2Ti_6O_{14}$/Li half cell. A reversible insertion of three lithium ions per unit formula was achieved due to the occurrence of vacant sites within the 3D-type structure [2,4]. The energy to fill these vacant sites is dependent on the geometry of the latter leading to insertion reactions at different voltages, i.e., plateau at 1.3 V and below this plateau [4]. Finally, the absence of a voltage plateau above 1.5 V, which may arise from the presence of TiO_2 or $Li_4Ti_5O_{12}$ impurities, ascertained the phase purity of the $SrLi_2Ti_6O_{14}$, in accordance with the XRD analysis.

At 100 mA g^{-1} current density (~1 C rate), the cycling behavior was stable over 100 cycles (Fig. 5). Both gravimetric (mAh g^{-1}) and volumetric (mAh cm^{-3}) capacities were determined. The volumetric capacity was calculated from the product of the gravimetric capacity and the packing density. The $SrLi_2Ti_6O_{14}$/Li half cell retained a capacity of 102 mAh g^{-1} (132 mAh cm^{-3}) after 100 cycles.

To further investigate the potential use of $SrLi_2Ti_6O_{14}$ as an anode, we investigated its coupling with a $LiMn_2O_4$ cathode. The charge and discharge curves of $LiMn_2O_4$/Li and $SrLi_2Ti_6O_{14}$/Li half cells are shown in Fig. 6A. The reported capacities correspond to those of the coin cells (1.6 cm^2), and are therefore expressed in mAh. The $LiMn_2O_4$ half cell displayed a smooth voltage profile corresponding to the delithiation/lithiation reaction within the spinel structure, leading to a reversible capacity of 103 mAh g^{-1} (3–4.3 V voltage window). The full cell $LiMn_2O_4$/$SrLi_2Ti_6O_{14}$ was charged/discharged over a potential range between 1.5 and 3.5 V (Fig. 6B). This resulted in a 2.7 V battery, which is a higher voltage than the 2.5-V $LiMn_2O_4$/$Li_4Ti_5O_{12}$ system [9].

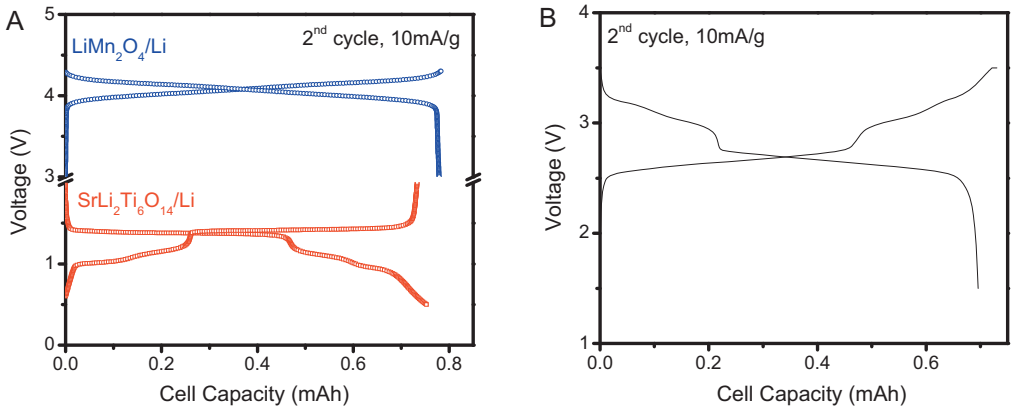

Fig. 6. (A) Typical voltage profile of $SrLi_2Ti_6O_{14}$/Li and $LiMn_2O_4$/Li half cells. (B) Charge and discharge curves of $LiMn_2O_4$/$SrLi_2Ti_6O_{14}$ full cell cycled between 1.5 and 3.5 V under 10 mA g^{-1}. The full cell is anode limited.

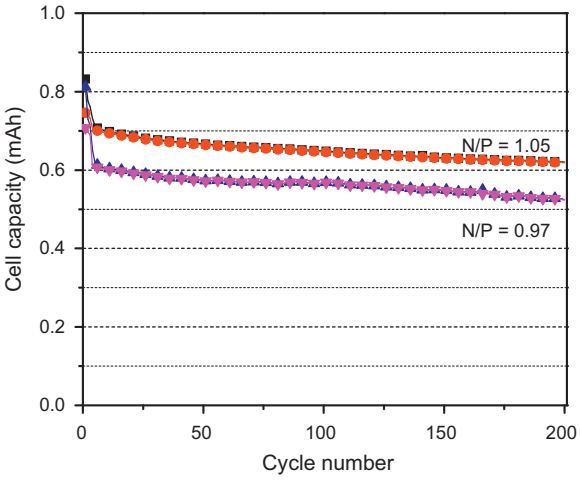

Fig. 7. Cycling behavior of $LiMn_2O_4/SrLi_2Ti_6O_{14}$ full cell cycled between 1.5 and 3.5 V at 100 mA g^{-1}.

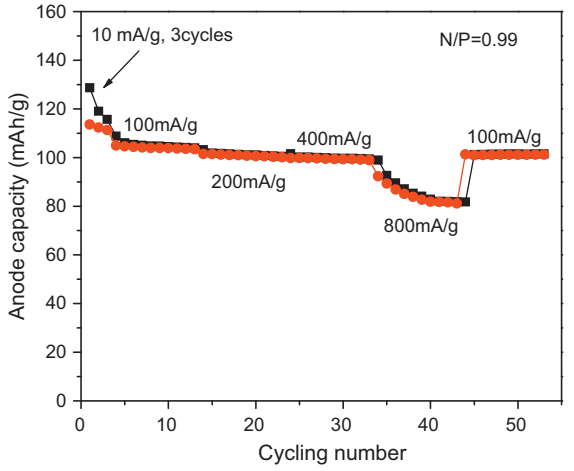

Fig. 8. Rate capability of $LiMn_2O_4/SrLi_2Ti_6O_{14}$ full cell cycled between 1.5 and 3.5 V.

Lithium-ion cells containing graphite materials are designed with a cathode-limited configuration in order to limit the source of lithium and, hence, to prevent lithium plating at the anode side. The high operating potential of $SrLi_2Ti_6O_{14}$ renders lithium plating unlikely, which suggests that flexible cell designs are possible. In our case, the $LiMn_2O_4/SrLi_2Ti_6O_{14}$ cell had been designed with both anode- and cathode-limited configurations. Fig. 7 shows the cycling performances of cells having negative-to-positive capacity ratios of N/P = 0.95 and 1.05. Both cell configurations exhibited excellent cycling behavior at the 1 C rate with only around 10% capacity loss after 200 cycles. The rate capability of the anode-limited $LiMn_2O_4/SrLi_2Ti_6O_{14}$ cell is displayed in Fig. 8. This cell was cycled at rates from 10 mA g^{-1} to 800 mA g^{-1}. The cell demonstrated excellent capacity retention with increasing rates up to 400 mA g^{-1}. At 800 mA g^{-1}, the cell started to show some capacity fading, but still maintained 80 mAh g^{-1} capacity delivered in 5 min. Thereafter, the cell was cycled at 100 mA g^{-1} and recovered its initial capacity.

4. Conclusion

Particles of $SrLi_2Ti_6O_{14}$ that are dispersable and possess high packing density have been synthesized using mesoporous TiO_2 as template and reactant. The prepared material reversibly inserts three lithium atoms per unit formula. When a $SrLi_2Ti_6O_{14}$ anode is combined with a 4-V cathode, the 2.7 V cell shows good cycling stability and rate capability. This makes $SrLi_2Ti_6O_{14}$ a promising anode for high power applications.

Acknowledgments

This research was funded by the U.S. Department of Energy, FreedomCAR and Vehicle Technologies Office. Argonne National Laboratory is operated for the U.S. Department of Energy by UChicago Argonne, LLC, under contract DE-ACO2-06CH11357.

References

[1] Z. Yang, D. Choi, S. Kerisit, K.M. Rosso, D. Wang, J. Zhang, G. Graff, J. Liu, J. Power. Sources 192 (2009) 588, and references therein.
[2] I. Belharouak, K. Amine, Electrochem. Commun. 5 (2003) 435.
[3] S.Y. Yin, L. Song, X.Y. Wang, Y.H. Huang, K.L. Zhang, Y.X. Zhang, Electrochem. Commun. 11 (2009) 1251.
[4] D. Dambournet, I. Belharouak, K. Amine, Inorg. Chem. 49 (2010) 2822.
[5] J.M. Tarascon, Nat. Chem. 6 (2010) 510.
[6] F. Cheng, Z. Tao, J. Liang, J. Chen, Chem. Mater. 20 (3) (2008) 667.
[7] D. Dambournet, I. Belharouak, K. Amine, Chem. Mater. 22 (2010) 1173.
[8] C. Boudaren, T. Bataille, J.P. Auffrédic, D. Louër, Solid State Sci. 5 (2003) 175.
[9] T. Ohzuku, K. Ariyoshi, Chem. Lett. 35 (2006) 848.